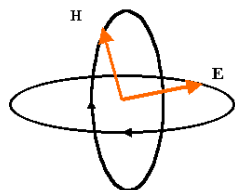


# GEMINI A&G POLARISATION MODULE OPERATIONAL CONCEPTS DEFINITION DOCUMENT V3.0



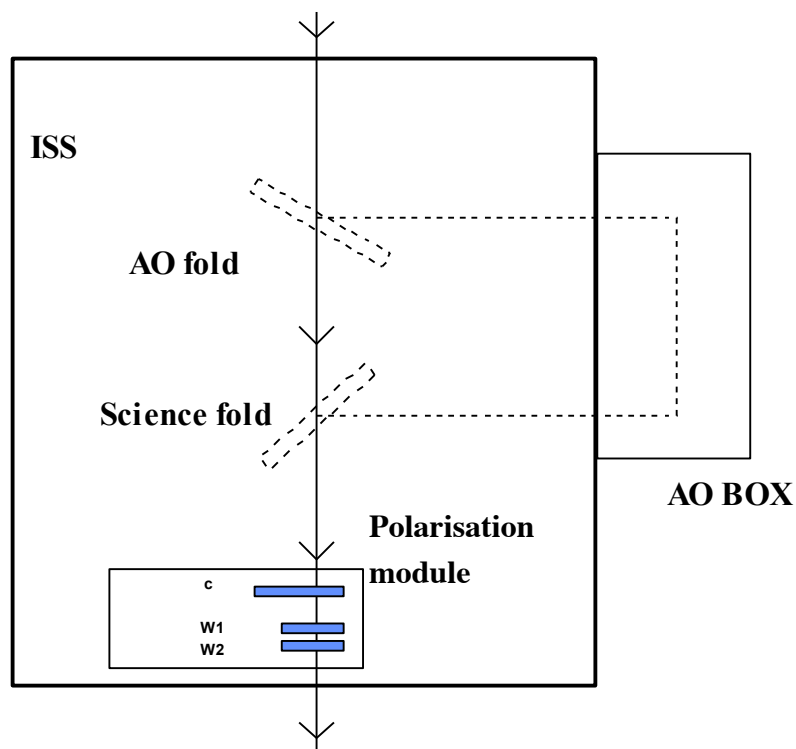
**James Hough**  
**David Aitken**  
**University of Hertfordshire**

<b>1. Introduction</b>	<b>2</b>	
<b>2. Scientific perspective</b>	<b>3</b>	
2.1 Producing polarised flux	3	
2.2 Polarimetry as a diagnostic tool	3	
<b>3. Required accuracy and precision</b>	<b>5</b>	
3.1 Degrees of polarisation	5	
3.2 Achieving a required accuracy	5	
3.3 Required precision	5	
3.3.1 Instrumental polarisation	5	
3.3.2 Polarisation efficiency	6	
3.3.3 Zero of position angle	6	
<b>4. The polarimetry module</b>	<b>8</b>	
4.1 Mechanical requirements	9	
4.1.1 Rotation modes	10	
4.1.2 Angular precision	11	
<b>5. The waveplates</b>	<b>13</b>	
5.1 Image wander	13	
5.2 Polarisation ripple	14	
5.3 Absorption bands	14	
5.4 Range and size of waveplates	14	
<b>6. Modes of Operation</b>	<b>16</b>	
<b>7. Interfaces to the Gemini systems</b>	<b>17</b>	
7.1 Physical	17	
7.2 Optical	17	
7.3 Control system	17	
7.4 Online data reduction	17	
<b>8. Requirements for each instrument</b>	<b>19</b>	
8.1 Analysers	19	
8.2 Masks	20	
<b>References</b>	<b>21</b>	
<b>Annexe A</b>	<b>Scientific Case</b>	<b>22</b>
<b>Annexe B</b>	<b>Alternative modulators</b>	<b>30</b>
<b>Annexe C</b>	<b>Materials for analysers</b>	<b>32</b>

## 1. Introduction

This document sets out the way a Polarisation Module will be used to provide linear and circular Polarimetry Modes for all Gemini Imagers and Spectrometers (except for Michelle which will employ an independent system). It will present the scientific cases, relate these to the requirements, and discuss the key functional and performance requirements that the Module must meet. It will identify and discuss the key operational scenarios, especially emphasising those requirements it will place on other parts of the Gemini system. It is assumed that waveplates will be used as the polarisation modulators, although alternative modulators are described in an Annexe.

Although primarily concerned with the Polarisation Module the document will make reference to the polarisation analyser and mask requirements for each instrument.



**Gemini ISS showing location of Polarisation Module**

Throughout this document, requirements and goals are generated from the concepts defined in the text. These are highlighted in boxes and numbered using a system dividing the requirements into the following categories:

- 1.n relate to telescope, A&G unit and polarisation unit interfacing
- 2.n relate to polarisation unit functions
- 3.n relate to polarisation unit performance
- 4.n relate to instrumentation
- 5.n relate to telescope system requirements

## 2. Scientific Perspective

There are few, if any, areas of astronomy where polarimetry does not or could not play a key role, ranging from planetary surfaces to distant active galaxies. This applies to observations covering the whole of the electromagnetic spectrum.

### 2.1 Producing polarised flux

#### *Intrinsic mechanisms:*

- electrons with low values of  $v/c$  in a magnetic field produce cyclotron radiation (circularly polarised)
- relativistic electrons produce synchrotron radiation (linearly polarised), with  $\underline{E}$  perpendicular to  $\underline{B}$
- in *emission* aligned grains (grain short axis parallel to the local magnetic field) produce polarisation with  $\underline{E}$  perpendicular to  $\underline{B}$
- Zeeman-split spectral lines are circularly polarised.

#### *Secondary mechanisms:*

- scattering off electrons or dust grains produces linear polarisation with  $\underline{E}$  perpendicular to the scattering plane for electrons and for dust grains whose size is small compared to the wavelength of radiation
- scattering of linearly polarised radiation off non-Rayleigh particles produces circular polarisation
- scattering of radiation (of any state) off aligned grains produces circular polarisation
- radiation passing through a medium of aligned dust grains (grain short axis parallel to the local magnetic field) produces polarisation by dichroic *absorption* with  $\underline{E}$  parallel to  $\underline{B}$ .

### 2.2 Polarimetry as a diagnostic tool

Polarimetry can provide the following information:

- presence of *synchrotron radiation* (linear polarisation) for core-dominated radio sources
  - ◊ doppler-boosted emission from *relativistic jets*, characterized by high and variable polarisation
- presence of *cyclotron radiation* (circular polarisation) produced by electrons in a magnetic field with most power generated at the gyration frequency for electron speeds that are low, relative to the velocity of light, while higher harmonics are produced as the velocity increases
- scattering (linear and circular polarisation)
  - ◊ view *usually obscured regions*
  - ◊ study the geometrical and velocity relationship between source, scatterer and observer *without spatially resolving the source*
  - ◊ comparison of total and (scattered) polarised *provides views of a source from different angles*
  - ◊ whereas linear polarisation is dominated by the *last scatter*, circular polarisation usually depends on the polarisation state of the last-scattered photon and hence provides information on the *previous history of that photon*
  - ◊ grain properties can be determined from the wavelength dependence of linear and/or circular polarisation.

- magnetic fields
  - ◇ linear polarisation, produced in absorption by the passage of radiation through aligned grains, or produced in emission from aligned grains, gives the direction of the magnetic field, as projected on to the sky plane
  - ◇ circular and linear polarimetry of Zeeman-split lines can give magnetic field strengths and directions, with the latter parallel to the line of sight
- spectral components
  - ◇ different components can be separated as they usually have a different spectral dependence of polarisation and different polarisation position angles
  - ◇ the polarised flux spectrum gives directly the spectrum of a polarised source diluted with unpolarised flux (e.g. a blazar with star light from a host galaxy).

**Annexe A** gives a number of more detailed examples of the science that can be carried out with Gemini polarimeters.

### 3. Required Accuracy and Precision

#### 3.1 Degrees of polarisation

Degrees of polarisation that are of scientific interest can range from many tens of percent (for some blazars and for spatially resolved reflection nebulae) to  $\sim 0.1$  percent (for small angle scatters or where there is substantial dilution of polarised flux). Thus, in many situations polarimetry is a technique that can take particular advantage of large aperture telescopes. In the optical and in the near-IR, at moderate spectral resolution, observations are more likely to be source noise limited, with the limiting flux then scaling as the square of the telescope diameter, whereas the limiting flux scales only as the telescope diameter for sky-limited observations.

#### 3.2 Achieving a required accuracy

For a dual-beam polarimeter, to obtain a 0.5% absolute uncertainty in the degree of polarisation a S/N ratio of 300:1 in total flux is required. For the source-limited case this corresponds to  $8 \times 10^4$  photons or  $4 \times 10^4$  per Stokes parameter.

It is important to note that with a dual-beam system the accuracy obtained is a function of photon numbers only and thus accurate polarimetry of bright sources can be carried out during observing conditions that are too bad for almost any other type of quantitative observation.

#### 3.3 Required precision

In order to achieve high precision in polarisation measurements (better than 0.05%, assuming a requirement to achieve similar accuracies), there are a few basic requirements:

- the polarisation modulator should be placed before any non-symmetric reflections; this usually means the instrument is located directly at the Cassegrain focus
- the detector should see a fixed plane of polarisation; i.e. the modulator and analyser should produce changes only in light intensity
- the analyser should transmit both orthogonal components of polarisation so they can be recorded simultaneously (in principle a high precision polarimeter can be produced with a single-beam analyser but this then requires rapid modulation ( $\sim$ several Hz), which is unsuited to most optical and near-infrared array detectors).

##### 3.3.1 Instrumental polarisation

The first requirement (see above) ensures that instrumental polarisation (IP) is negligible. IP is the polarisation produced when observing a source of zero polarisation, and for the Gemini telescopes is anticipated to be  $\leq 0.05\%$ .

Typically a 45 degree reflection will produce a polarisation of  $\sim 5\%$  in the visible (Gehrels 1960) and 0.5% in the near-infrared (Dyck, Forbes & Shawl, 1971), although the actual values depend on the nature of the reflecting surface and may change with time. As long as the IP is small, it is added vectorially to the Stokes vector and can therefore be subtracted off in the same way. For large IP and large source polarisation, a full Mueller matrix treatment is needed.

The IP can be determined by observation of unpolarised stars. Lists of such standards, generally nearby F&G type stars, are available for the optical and near-infrared. Also, as the

A&G and instrument will be rotated so as to remain fixed relative to the sky, the source polarisation will rotate relative to the telescope and hence the contribution to the IP of the latter can be determined independently.

A more troublesome problem is when the telescope acts like a *retarder*, rather than a *polariser*, and converts, for example, linear polarisation into circular polarisation. Like other forms of IP, the effect is small when the beam suffers no oblique reflections prior to the analyser.

There are cases where the effect of (small) IP may be unimportant. For example, measuring high degrees of polarisation or in the case of velocity resolved spectropolarimetry where the IP, which changes only slowly with wavelength, will be effectively constant across a spectral line and thus simply add to the continuum polarisation.

**Requirement 1.1:** For highest precision ( $P \leq 0.05\%$ ), the polarisation module should be before any non-symmetric reflections.

### 3.3.2 Polarisation efficiency

The normal method of measuring polarisation efficiency is to use standard polarised stars or a standard calibrator. The latter is preferable as standard stars have generally low degrees of polarisation ( $\sim 5$  percent or less at V, and smaller at shorter and longer wavelengths), whereas calibrators are available which can produce polarisations of 100%.

Introducing a highly polarised calibrator into the beam can also be a rapid way of checking that the polarimeter is operating correctly, at least for linear polarisation. Standard circular polarisers are less easy to include.

**Requirement 2.3:** For ease of measuring polarising efficiency and checking that a polarimeter is fully functional a set of 3 calibrators, that can be automatically deployed, is required to cover the wavelength range of Gemini polarimeters

### 3.3.3 Zero of position angle (PA)

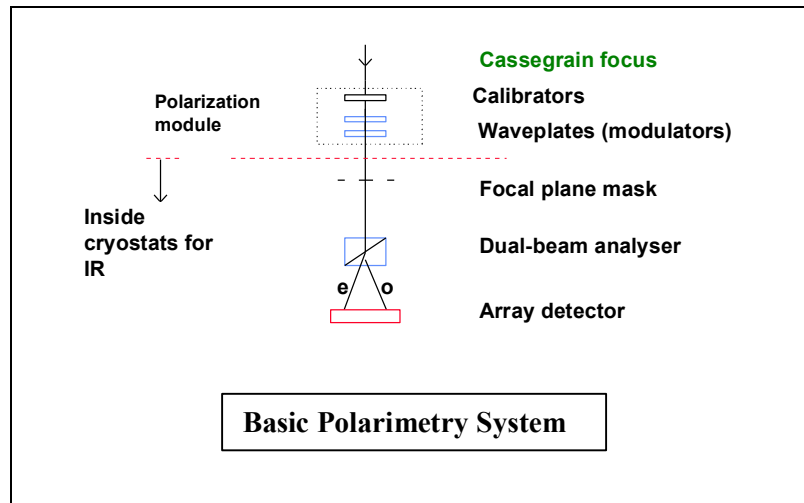
The polarisation PA is usually measured with respect to some instrumental zeropoint, which can depend on wavelength (e.g. the fast axis of a multi-element waveplate can vary by a few degrees over its useful wavelength range). This has to be converted to a reference direction on the celestial sphere.

Specialised methods have been established to calibrate the PA, e.g. using a reversible Polaroid suspended in front of a nearly horizontal telescope (Gehrels and Teska 1960), or from the terrestrial blue sky at the zenith (Konnen et al 1993). It is sufficient, however, to use the polarisation efficiency calibrators (see 3.3.2) to determine any wavelength dependence of PA for each instrument, and polarised standard stars to relate these PAs to the celestial sphere.

Polarised standards (see the list of Whittet et al 1992, and references therein) are available for wavelengths between 0.3 and 2.5 $\mu\text{m}$ , but at longer wavelengths the degrees of polarisation for these stars are generally small. Stars embedded in dark clouds, with high extinction, have been used for longer wavelengths but there may be some local polarisation produced by reflection nebulosity around the star, and thus the polarisation may be aperture dependent, and may also be variable.

## 4. The polarimetry module

Thus far the description could apply to almost any type of polarisation modulator. Hereafter it is assumed that the modulators are waveplates. **Annexe B** gives a brief description of alternative modulators.



For **linear** polarimetry a single half-wave retarder is required. Images are recorded at four positions of the waveplate ( $0^\circ$ ,  $45^\circ$ ,  $22.5^\circ$ , and  $67.5^\circ$ ). If a dual-beam analyser is used both orthogonal components of polarisation are recorded simultaneously, and the accuracy of polarisation is not affected by changes in atmospheric transparency between the different waveplate positions.

For **circular** polarimetry both quarter-wave and half-wave retarders are often used together. In most astrophysical situations degrees of circular polarisation are generally low, and are often accompanied by much larger degrees of linear polarisation. In order to eliminate systematic errors produced by measuring some of the linear polarisation as circular, a half-wave retarder can be rotated continuously in front of the stepped quarter-wave retarder. Exposure times, at each position of the quarter-wave retarder, should be an integral number of one-quarter the period of the mechanical rotation of the half-wave retarder. Exposures are needed at  $0^\circ$ ,  $90^\circ$ ,  $45^\circ$  and  $135^\circ$ , or at just two positions of the quarter-wave retarder, separated by  $90^\circ$ , provided these correspond to positions of maximum modulation. These positions can be determined by using a circularly polarised (calibration) source and noting the angles, separated by  $90^\circ$ , at which the most circular is measured.

If the error in determining the angle(s) of maximum modulation is  $\Delta\theta$ , then the efficiency of measuring circular polarisation is reduced to  $\cos 2\Delta\theta$ . For superachromatic quarter-wave retarders (see section 5), the fast axis of the waveplate is wavelength dependent, with a swing of a few degrees between  $0.3$  and  $1\mu\text{m}$ . Taking  $\Delta\theta$  as 3 degrees, the efficiency of measuring circular polarisation will drop to  $\sim 99.6\%$  for some parts of the spectrum, a negligible change.

The need to use a rotating half-wave retarder has not always been clearly stated in the literature. When using a dual-beam analyser, any linear polarisation that is present will only be measured as circular when the angles at which exposures are made are not correctly spaced (see section 4.1.2 for more details). Any difference in retardance of the waveplate

from  $\lambda/4$  only affects the cross-talk when the exposures are made at the wrong angular separations of the plate.

There is another problem that might occur if a rotating half-wave retarder is not used prior to the stepped quarter-wave retarder. For a highly linear polarised source, the quarter-wave retarder converts linear-to-circular, so the radiation after the quarter-wave retarder is highly circularly polarised. If an analyser is the next element then there is no problem. However, if there are a number of optical elements between the waveplate and the analyser, and some of that optics has birefringence, thus converting circular to linear polarisation which will be detected by the analyser.

#### 4.1 Mechanical requirements

The polarisation hardware must locate on module one of the Gemini A&G facility. Disruption to the existing equipment must be minimised.

As the same module will be used with all Gemini instruments a module containing a number of waveplates will minimise the number of changes that have to be made. Also, two waveplates may be used together for circular polarimetry (but see previous section).

Waveplates should be introduced into and withdrawn from the module with the minimum disruption (e.g. by using the port-hole in the bottom of the ISS when the bottom instrument is removed).

When not in use, the polarimetry optics must be withdrawn completely from a 7 arcmin diameter fov. As a goal, it should be withdrawn completely from the 10 arc min diameter fov of Gemini. The waveplates should retract into a dust cover when not deployed.

All the waveplates should fit into the module with their fast axes aligned in the same direction (with a precision of a quarter of a degree). This then gives the same zero of position angle for each plate.

The waveplates must not be able to rotate in the holders.

Each waveplate should be encoded so that the software can check that the correct waveplate is being used with each instrument/wavelength range.

The on-axis centering should be better than  $\pm 0.5\text{mm}$ .

**Requirement 1.2:** When not in use the polarimetry module must not vignette a 7 arcmin diameter fov.

**Goal 1.2:** When not in use the polarimetry module should not vignette a 10 arcmin diameter fov.

**Requirement 1.3:** The waveplates should retract into a dust cover when not deployed.

**Requirement 2.4:** the Polarisation Module will need to operate two waveplates together.

**Goal 2.4:** The Module should contain at least three waveplates that can be accessed and operated remotely.

**Requirement 3.1:** Waveplates should be introduced and withdrawn with the minimum disruption.

**Requirement 3.2:** The on-axis centring should be better than  $\pm 0.5\text{mm}$ .

**Requirement 3.3:** Waveplate identification to be electronically encoded.

**Requirement 3.4:** Waveplates must not be able to rotate in their holders.

**Requirement 3.5:** The waveplate optical axes to be aligned in the same direction with a precision of a quarter degree.

#### 4.1.1 Rotation modes

The waveplates should be capable of being rotated either continuously or in step-and-stare mode. The direction of rotation should not be changeable except under engineering control and when in observing mode the direction should always default to the same sense. This prevents changes in the direction of rotation of the polarisation position angle, and prevents any backlash problems. Sensors, attached to the waveplate assembly and not to the motor, should be used to set the waveplates to their usual operating positions of 0, 22.5, 45, 67.5, 90 and 135 degrees. There is no requirement for the 0-degree position to be fixed relative to the celestial sphere as the zero of polarisation PA will be determined independently. Other angular positions, in steps of a half-degree, or less, should be available by offsetting from the 0-degree position. To prevent optical cross-talk the sensors should either be magnetic or if optoswitches are used they should be powered off when the correct position is reached.

In step and stare mode rotation can start immediately after an exposure has been completed, and the speed of rotation should be sufficient to minimise dead-time between exposures so as to maximise the observing efficiency. There are two scenarios with, in both cases, read-out times of IR arrays assumed to be  $\ll 1$  sec and for optical arrays  $\sim 1$ -2sec:

- (i) Bright standard polarised stars: on-chip and read-out assumed to be  $\sim 1$ sec for each of the four waveplate positions. For a rotation period of  $\tau$  sec, the time to complete the sequence  $0^\circ, 45^\circ, 22.5^\circ, 67.5^\circ$ , is  $1.2\tau$  (assuming rotation back to  $0^\circ$  takes place in between observations). Thus the observing efficiency is  $4/(4+1.2\tau)$ , or 77%, 63%, 40% and 25% for  $\tau = 1, 2, 5$  & 10 sec respectively.
- (ii) Programme object: on-chip and read-out time assumed to be 60s per waveplate position. Observing efficiency is  $240/(240+1.2\tau)$ , or 99.5%, 99%, 98% and 95% for  $\tau = 1, 2, 5$  & 10 sec respectively.

Given that the number of standard stars that will be observed in any one night is likely to be small, a reasonable requirement for the minimum rotation period ( $\tau_{\min}$ ) is 5s. This will give an observing efficiency of  $\sim 40\%$  for bright stars and 98% for typical programme objects. There should be a goal for  $\tau_{\min}$  of 4s.

Continuous rotation is required for circular polarimetry (but see start of section 4), unpolarised flat-fields, and there may be other - as yet unforeseen uses. For this mode  $\tau_{\min}$  should be an integral number of half-seconds, uniform to 1 part in 200 and with a long-term (1 hour) precision of 1%. The period of rotation  $\tau$  should be programmable, ranging from  $\tau_{\min}$  to  $10\tau_{\min}$  in steps of  $0.5\tau_{\min}$ . For circular polarimetry or unpolarised flat-fields exposure times (including co-adds) should be multiples of a quarter of the rotation period. Alternatively, but with less efficiency, a sufficiently large number of rotations can be used such that any non-complete rotation becomes negligible (e.g. to reduce the polarisation of a flat field by a factor  $n$  requires  $(n/16r)$  rotations where  $r$  is the rotation rate in Hz).

Motors should be put in standby mode during observations to limit the heat dissipation, while still retaining sufficient torque to stop any rotation.

**Requirement 3.6:** Waveplates to be rotated continuously or in step-and-stare mode.

**Requirement 3.7:** Sensors, attached to the rotating assembly, should be used to define the usual operating positions: 0, 22.5, 45, 67.5, 90 and 135 degrees.

**Requirement 3.8:** The sensors should be magnetic or, if optical, should be powered off when the operating position has been reached.

**Requirement 3.11:** Any angular position, in steps of a half-degree or less, should be available by offsetting from the 0-degree position. This position can be arbitrary with respect to the celestial sphere.

**Requirement 3.14:** The minimum rotation period ( $\tau_{\min}$ ) should be an integral number of half-seconds.

**Requirement 3.15:**  $\tau_{\min} = 5$  sec.

**Goal 3.15:**  $\tau_{\min}$  to be 4 sec.

**Requirement 3.16:** Rotation periods should be programmable with  $\tau$  ranging from  $\tau_{\min}$  to  $10\tau_{\min}$  in steps of  $0.5\tau_{\min}$ .

**Requirement 3.17:** Continuous rotation should be uniform to 1 part in 200 and with a long-term precision of 1%.

**Requirement 3.18:** Motors to be in standby mode when stationary to reduce heat dissipation, but to retain sufficient torque to stop any slippage.

#### 4.1.2 Angular precision

##### (a) Linear polarisation

A random jitter in the angular position of the waveplate translates into an uncertainty in the position of angle of polarisation (PA). For example, a square-wave jitter of  $\pm 1^\circ$ , gives a variance in the PA of  $\sim 0.64^\circ$ .

A systematic error in the position of the waveplate will result in a shift in the zero of PA, which can be taken out in the calibration. Incorrect spacing of the positions at which exposures are made will affect the polarisation efficiency, which again will be determined through calibrations. In any case, the effect is very small for angle offsets up to a few degrees.

##### (b) Circular polarisation (note that quarter-wave retarders are not in the baseline)

If exposures are not made at the correct angular settings of the (stepped) quarter-wave retarder severe cross-talk can occur. For example, in the presence of 100% linear polarisation in the U Stokes vector, a  $0.1^\circ$  offset in the zero-degree position leads to a 0.2% circular, a  $0.2^\circ$  offset to 0.3% circular, a  $1^\circ$  offset to 1.7% circular and a  $5^\circ$  offset to 8.6% circular

polarisation. The cross-talk is proportional to the degree of linear polarisation. A small jitter (1 degree or more) in the positioning of the waveplate will also lead to the same problem. For the highest precision, circular polarimetry should be carried out in conjunction with a continuously rotating half-wave retarder, thus eliminating the linear polarisation. The rejection ratio is not a strong function of the retardance of the  $\lambda/2$  plate, with a retardance of  $175^\circ$  leading to 0.02% circular, and a retardance of  $150^\circ$  giving only 0.6% circular, both calculated for a  $5^\circ$  error in the position of an exposure and a 100% U.

**Requirement 3.12:** Each of the waveplate operating positions, defined in section 4.1.1, should be accurate to better than 0.2 degrees relative to the zero-degree position.

**Requirement 3.13:** Intermediate waveplate operating positions, should be accurate to better than 0.2 degrees relative to the zero-degree position.

## 5. The waveplates

Waveplates have the advantage that it is possible to make the plates achromatic, or even superachromatic, by using combinations of plates and by using different materials. The nomenclature can be confusing: superachromat is a term commonly applied to plates that cover 0.3 to 1.1 $\mu\text{m}$ , although it is possible to make plates achromatic from 0.3 to 2.5 $\mu\text{m}$ ; the term achromat has been used to describe plates covering 1.0 to 2.5 $\mu\text{m}$ . Waveplates will accept a wide angular beam (e.g. the polarisation efficiency of a superachromat is still  $\geq 98\%$  for a f/16 beam), and generally have good transmission although careful cementing or the use of optical matching oils is needed when multiple plate retarders are used.

Any waveplate will have some departure from a true  $\lambda/2$  or  $\lambda/4$  retardance. For the case of a superachromat, covering 0.3 to 2.5 $\mu\text{m}$ , the maximum departures from a  $\lambda/2$  or  $\lambda/4$  retardance are 5% and 10% respectively (B Halle design), which leads to a reduction in polarisation efficiency (see below), which can be easily measured and accounted for in data reduction. The effect of the change in the orientation of the optic axis with wavelength of a few degrees, that occurs with (super)achromatic waveplates, can be easily corrected in the data reduction.

### (i) a $\lambda/2$ retarder

For a 5% error in retardance, the modulation efficiency is reduced by only  $\sim 0.9\%$ . A potentially more significant problem is that in the presence of a 100% circular polarisation, a spurious linear polarisation of  $\sim 9\%$  would be measured. Apart from AM Her binaries, objects usually have much higher linear than circular polarisation and thus the cross-talk is unlikely to be a problem in practice.

### (ii) a $\lambda/4$ retarder

For a 10% error in retardance, the modulation efficiency is reduced by only  $\sim 1.5\%$ . As noted in section 4, a non-perfect  $\lambda/4$  retarder does not in itself cause any linear polarisation to be measured as circular.

### 5.1 Image wander

The main disadvantage of waveplates is that they have to be mechanically rotated and this can lead to image wander:

- (i) when the plates have an error angle  $\varphi$  in plane parallelism, plate thickness  $d$ , distance to focus of  $D$ , then the radius of the error circle  $r$  at focus is given by:  

$$\mathbf{r} = \mathbf{D} \varphi (\mathbf{n}-1) + \mathbf{d} \varphi (\mathbf{1}-1/\mathbf{n})$$
; second term applies only if the tilt is on the upper surface.  
 For a goal of  $r < 0.050$  arcsec (f/16 focus, plate scale 1.6 arcsec/mm,  $r \sim 30\mu\text{m}$ ),  $D \sim 750\text{mm}$ ,  $d \sim 20\text{mm}$  and  $n \sim 1.5$  (see section 7.2),  $\varphi < 30\text{arcsec}$ . Note that the second term is negligible.
- (ii) when the rotation axis is not normal to the plate, with an error of  $\varphi$ :  

$$\mathbf{r} = \mathbf{d} \varphi (\mathbf{1}-1/\mathbf{n})$$
; giving a requirement of  $\varphi < 16\text{arcmin}$  for the same constraint.
- (iii) when the rotation axis is not parallel with the telescope axis, the image shift at focus is the same as (ii) above, but it is fixed after the insertion of the plate and is independent of rotation.

Alternatively, for step-and-stare mode, any image wander can be corrected for in real-time by moving the telescope by offsets that have been previously calculated for each of the waveplate positions.

## 5.2 Polarisation ripple

Another problem when using waveplates for spectropolarimetry is the occurrence of a ripple in the polarisation spectrum at moderate to high spectral resolutions. Multiple interference between the different surfaces of composite waveplates appears to be responsible, with the beats occurring through interference effects at slightly different optical spacings (the ripple spacing is proportional to  $\lambda^2$ ). The effect is most marked at UKIRT where the waveplates have air spacings resulting in larger reflections at each interface. The plates were not cemented as this was thought to be difficult for plates with a diameter of 95mm. A possible remedy is to include an optical oil between the plates to provide better optical matching.

At present the ripple is removed by doing a Fourier Transform of the spectrum, removing the power at the ripple frequencies and then doing the inverse transform. This process works well but it would be sensible to minimise the effect or to have an algorithm which automatically removes the ripple from the data. Although the cause of the effect appears to be understood in general terms, a detailed analysis of the effect for particular waveplates needs to be carried out.

## 5.3 Absorption bands

Hydrocarbons in the cements used in the construction of waveplates and Wollaston prisms can produce significant absorptions in the near-infrared. For example using CGS4+IRPOL, on UKIRT, produces a deep absorption band between 3.35 and 3.4  $\mu\text{m}$ .

## 5.4 Range and size of waveplates

Separate retarders are usually needed to cover 0.3 to 1.1 $\mu\text{m}$ , 1.0 to 2.5 $\mu\text{m}$  and each of the L and M bands. However, single retarders can be produced to cover 0.3 to 2.5 $\mu\text{m}$ , with polarisation efficiency greater than 99%. The L and M retarders should be first-order plates which act as a single order plate with respect to the variation of retardance with wavelength ( $P_r \sim \sin(\pi/2 \cdot \lambda_0/\lambda)$ ), temperature and angle of incidence. Multiple order plates should be avoided.

The free aperture of the waveplates should ideally cover the field of view of all the instruments. In practice this may not be possible, at least not with single crystals. For these, the maximum diameter plates for 1-2.5 $\mu\text{m}$  and for the L and M bands, are  $\sim 95\text{mm}$ , and probably no more than  $\sim 65\text{mm}$  for 0.3 to 1.1 $\mu\text{m}$  or 0.3 to 2.5 $\mu\text{m}$ <sup>1</sup>. However, mosaics can be made and B Halle have constructed a 3x3 mosaic for the ESO VLT, with each section 45x45mm. The dead-space between each section is  $\sim 2\text{mm}$ . In principle even larger mosaics could be constructed. The fovs of the instruments are shown in Table 1. Waveplates of 65mm clear aperture would be sufficient for the finest scale of NIRI, for 88% of the long camera slit and 55% of the short camera slit of NIRS, for 88% of the HROS slit, and for 28% of the long-slit mode of GMOS. Waveplates of 95mm clear aperture would be sufficient for all but the coarsest scale of NIRI, for the whole slit of the long camera and most of the slit of the short camera of NIRS, for HROS, and for 40% of the long-slit mode of GMOS.

<sup>1</sup> a 0.35 $\mu\text{m}$  to 2.5 $\mu\text{m}$   $\lambda/2$  single piece waveplate, with clear aperture of 95mm, is being constructed for Hough by B Halle for a different project, although delivery (as of Jan 7 2000) is delayed.

Instrument	Fov (arcsec)	fov (mm)	Notes
------------	--------------	----------	-------

NIRI	20, 50, 120	57, 74, 113	pixel scales 0.02, 0.05, 0.12 arcsec
NIRS	50 (long camera) 150 (short camera)	74 129	
HROS	60	79	long-slit mode
GMOS	330x330	229x229	long-slit mode
OIWFS	210	163	

Table 1: Fields of view of the Gemini instruments. The diameter of the fov in mm is calculated assuming a distance of 0.73m from the focal plane, and a scale of 1.8 arcsec/mm. At this distance a diameter of 46mm is required for an unvignetted fov for a point source.

Also shown in Table 1 is the fov of the OIWFS. In order to maximise the opportunity of finding field stars for the tip-tilt secondary the full fov of the OIWFS, with a clear aperture of ~165mm diameter, is required. As single crystal plates of this size are not available either mosaics must be used or the waveplates must be surrounded by a transparent ring (possibly fused silica) of diameter 165mm. Because of the large size, the thickness of this size of ring may need to be larger than the thickness of the waveplate, requiring the use of a compensating additional glass plate (fused silica) to equalise the optical depths of the waveplate and the ring. Unequal optical depths would produce significant dead-space as the unvignetted diameter of a point source is 46mm at the position of the polarisation module. In this case the ring would contribute no additional fov as the width of the ring is less than the image size.

**Requirement 2.1:** A single (superachromatic) waveplate to cover 0.3 to 1.1 $\mu$ m and a single (achromatic) waveplate to cover 0.9 to 2.5 $\mu$ m; first-order plate to cover the L band (M-band plates are not in the baseline).

**Goal 2.1:** A single (superachromatic) waveplate to cover 0.3 to 2.5 $\mu$ m.

**Requirement 2.2:** Waveplates to provide  $\lambda/2$  retardances (quarter-wave retarders - for circular polarimetry - are not in the baseline).

**Requirement 2.5:** Waveplate clear apertures to be minimum of 95mm.

**Requirement 2.6:** Waveplates to produce beam-wander of less than 0.050arcsec at the focal plane by their wedge-angle being less than 0.5 arcmin.

**Requirement 2.7:** Rotation axis of waveplate to be normal to the waveplate to within 16 arcmin so beam wander is less than 0.050arcsec.

**Requirement 2.8:** Clear aperture of rotating assembly to be 165mm. Optical thickness of waveplate and clear aperture to be uniform to 1%.

## **6. Modes of Operation**

Polarimetric observations are relatively straightforward, with a number of normal exposures taken at each of the (4) waveplate positions. A typical observing sequence is given below. It is assumed that the imager or spectrometer has already been checked out. Flat fields are normally carried out with the analyser in position. Ideally the flat field source should be unpolarised and this can be achieved by continuously rotating a half-wave retarder (see section 4.1.1). Alternatively exposures can be taken at each waveplate position.

(a) Linear polarisation:

- the appropriate waveplate is moved into the beam (software checks that the plate is the right one for the instrument/wavelength range to be used)
- the calibrator (giving a known and high polarisation) is introduced into the beam
- exposures of a bright unpolarised star are taken at each of the four waveplate positions; on-line data reduction checks that the polarisation is correct
- exposures taken of a polarised standard; on-line data reduction checks that the polarisation and PA of polarisation are correct (note that the PA will have been already calibrated)
- objects from the source list can be observed; on-line data reduction essential to check on progress (check can be made to see if expected S/N will be achieved in estimated time); for imaging polarimetry the telescope may need to be moved when the source is more extended than the slot in the focal plane mask
- flux standards also observed (usually done in polarimetry mode, but is not of course essential)

(b) Circular Polarisation (note that quarter-wave retarders are not in the baseline):

Essentially the same sequence is carried out although if the (2) positions of maximum modulation are known exposures are only needed at these positions, thus doubling the observing efficiency. Exposure times (including co-adds) are set so they are multiples of a quarter of the rotation period of the continuously rotating half-wave retarder.

## 7. Interfaces to the GEMINI systems

### 7.1 Physical

The polarimeter module hardware must locate within the A&G unit with minimal disruption.

The control hardware will be mounted external to the ISS. If practicable the A&G control hardware will be utilised to drive the various mechanisms.

### 7.2 Optical

When the polarimeter module is in the telescope beam it will change the telescope focus. The increase in focus distance is  $d(1-1/n)$ , where  $d$  is the physical thickness of the plate and  $n$  the refractive index. The smallest value of  $d$  is  $\sim 9\text{mm}$ , for the L-band plate made of  $\text{MgF}_2$ , with  $n \sim 1.35$ , giving an increase in focus distance of  $2.3\text{mm}$ . The largest value of  $d$  would be  $\sim 20\text{mm}$ , for a superachromat covering  $0.3$  to  $2.5\mu\text{m}$ , made of magnesium fluoride and quartz ( $n \sim 1.35$  and  $1.5$  respectively), giving an increase in focus distance of  $\sim 5.7\text{mm}$ . For circular polarimetry, where two waveplates are used together, the largest increase in distance would be  $\sim 11.4\text{mm}$ .

With a polarisation calibrator in the beam, there would be an additional optical path length. For a ZnSe wiregrid polariser, typical thickness  $5\text{mm}$ ,  $n \sim 2.65$ , gives an additional  $3.1\text{mm}$  increase in focus distance.

The change in focus for the instrument, including the OIWFS, should be accommodated by a change in the telescope focus. However, the PWFS focus will need to be separately corrected. This might be achieved by using a glass plate, or plates, of suitable optical thickness in the PWFS filter wheel.

Every part of the polarimetry module, when not being used, must clear the full fov of Gemini.

### 7.3 Control System

The Gemini system has to be able to rotate up to two waveplates, either in continuous or step and stare mode. In step mode, rotation stops when the selected sensor switches, or when the stepper has moved a preset number of steps. The sense of rotation should be switchable in engineering mode, but always default to the same sense in observing mode.

In step-and-stare mode any beam wander resulting from the rotation of the waveplate can be corrected for by offsetting of the telescope.

### 7.4 Online data reduction

As polarisation is calculated from what are often small differences between exposures taken at different waveplate positions, it is essential that there is excellent online data reduction. Without that it is very easy to waste telescope time. See Berry & Gledhill 1998 for an excellent description of Starlink's comprehensive data reduction package for imaging polarimetry.

<b>Requirement 1.4:</b> Minimal disruption to the A&G hardware.
---

**Goal 1.4:** No disruption to the A&G hardware.

**Requirement 1.5:** The control hardware will be mounted external to the ISS.

**Goal 1.5:** The WFS control hardware will be utilised to drive the various mechanisms.

**Requirement 3.9:** Rotate one or two waveplates, either in continuous or step and stare mode.

**Requirement 3.10:** Sense of rotation should be switchable in engineering mode, but always default to the same sense in observing mode.

**Requirement 5.1:** In step-and-stare mode any beam wander resulting from the rotation of the waveplate can be corrected for by offsetting of the telescope.

**Requirement 5.2:** The Gemini telescope focus must be capable of increasing by up to 15mm.

**Requirement 5.3:** The PWFS focus needs to be mechanically adjustable by up to 15mm or a glass plate, or plates, of suitable optical thickness can be placed in the PWFS filter wheel.

**Requirement 5.4:** Online data reduction to give Stokes parameters for individual integration and running average (with uncertainties).

**Requirement 5.5:** The TCS must inform the relevant instrument when the GPOL is in position to make an observation.

## 8. Requirements for each instrument

Each instrument has to include a polarisation analyser and a focal plane mask. Although these are the responsibility of the instrument teams it is useful to include the requirements here.

### 8.1 Analysers

Two types of polarising prism are commonly used: calcite blocks, that produce a translational displacement between the e- and o-rays, and Wollaston prisms that produce an angular separation of the two beams.

Calcites have been used in a number of optical spectrographs placed below the spectrograph slit, with a beam displacement which is  $\sim 0.1$  x the calcite thickness. A simple calcite has the disadvantage that the two beams have different optical path lengths and therefore a different focus. This can be overcome by using a Savart plate, as in the ISIS spectropolarimeter on the WHT (Tinbergen 1992). Calcites cannot be used beyond  $2.0\mu\text{m}$  because of their large opacity to the o-rays. As these optical elements are placed in a non-collimated beam optical aberrations will normally be introduced but these can be minimised by having some optical power in the analyser. Also, the introduction of a calcite/Savart plate will change the focus.

Goodrich (1991) describes a modified Glan-Taylor calcite polarising beam splitter that produces a beam separation equal to the beam diameter, although the two beams have unequal path length.

Wollaston prisms have been used in the collimated beams of IR cameras and spectrometers (Hough et al 1994, 1996). The deviation of the 2 beams is given by  $\delta_{eo} = 2 (n_e - n_o) \tan\Omega$ , where  $\Omega$  is the prism angle, and  $(n_e - n_o)$  is the material birefringence. Double Wollastons, with twice the thickness and angular dispersion, can also be produced. Oliva et al (1996) give the separation of the two beams in arc seconds, expressed in sky-projected angles as  $2063(n_e - n_o) \tan\Omega \cdot D_p D_{\text{tel}}^{-1}$ , where  $D_p$  is the diameter of the pupil image inside the instrument (in centimetres) and  $D_{\text{tel}}$  is the telescope diameter in metres.

In selecting a material consideration has to be given to: transmission, the required beam separation and birefringence of materials, wavelength dependence of birefringence (images can become elongated in the polarisation dispersion direction when using broadband filters - the effect can be reduced by reducing the separation between the e- and o-beams), the ability to cement the (two) components of a Wollaston prism, and the ability to operate at low temperatures for infrared instruments. **Appendix C** gives information on possible materials for each instrument.

When using reflection gratings a problem can arise when the polarisation state of one of the beams is crossed with the polarisation axis of the grating, leading to significant loss of light and an imbalance between the two beams. There are two ways to reduce the effect. First, to have the polarisation states of both beams at 45 degrees to the polarisation axis of the grating, thus ensuring that the beams are balanced. Second, to use a quarter-wave retarder after the analyser, with its fast axis at 45 (and 135) degrees to the two orthogonal polarisations. This will convert the linear to circular polarisation.

**Requirements 4.1:** Two-beam polarising prisms to be used as analysers.

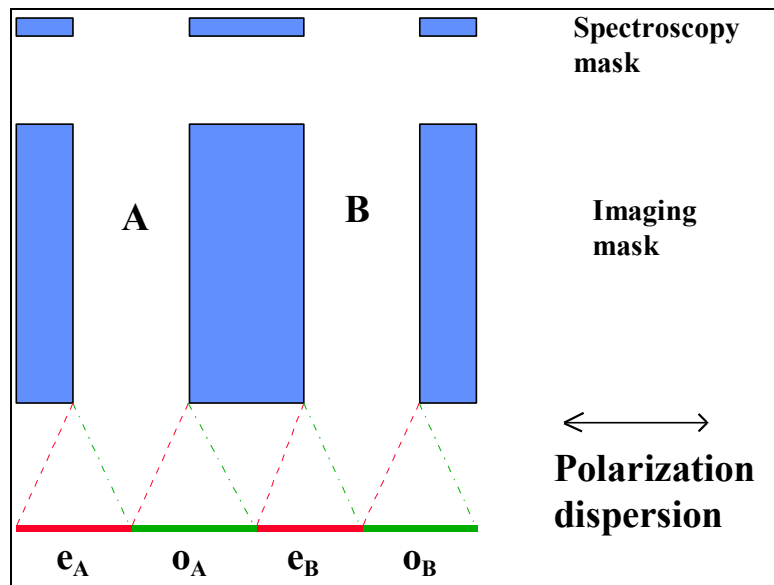
**Requirement 4.2:** With reflection gratings to have the two orthogonal polarisations making the same angle with the polarisation axis of the grating

**Goal 4.2:** With reflection gratings, to include quarter-wave retarders after the analyser

## 8.2 Masks

A focal plane mask is required so extended objects can be observed without overlapping the two beams from the dual-beam analyser. Below is shown a mask for imaging and for spectroscopy, used with a dual-beam analyser which gives a beam separation of one-quarter of the array. The separation of beams is a compromise between possible optical aberrations produced for large separations and cross-talk for too small a separation. Large separations are convenient as extended objects may be fully covered by one of the mask gaps and observations can be made with a single setting of the telescope.

**Requirements 4.3:** Focal plane grid masks, with spacings matched to the separation of the orthogonally polarised beams.



## References

- Berry DS & Gledhill TM, 1998 Starlink User Note 223.1, CCLRC/RAL
- Dyck, Forbes & Shawl 1971, *Ast J*, **76**, 901-915
- Gehrels 1960 *Ast J*, **65**, 466-469
- Gehrels T & Teska T M 1960, A Wollaston photometer, *Proc Astron Soc Pacific*, **72**, 115
- Goodrich R.W., 1991, High-efficiency "superachromatic" polarimetry optics for use in optical astronomical spectrographs, *Pub. Astron. Soc. Pacific* **103**, 1314-22
- Hough J.H., Peacock T. & Bailey J.A., 1991, A multiband two-beam optical and infrared polarimeter, *Mon. Not. Roy. Astron. Soc.* **248**, 74-8 et al
- Hough J.H., Chrysostomou A. & Bailey J.A., 1994, A new imaging infrared polarimeter, In *Infrared Astronomy with Arrays: The Next Generation*, ed. I.S.McLean, Astrophysics and Space Science Library **190** (Kluwer Academic Publishers, Dordrecht), pp. 287-9
- Konnen G P, Schoenmaker A A & Tinbergen J, 1993, A polarimetric search for ice crystals in the upper atmosphere of Venus, *Icarus* **102**, 62.
- Oliva E, Gennari L, Vanzi L, Caruso A & Ciofini M, 1996, Optical materials for near-infrared Wollaston prisms, A&A, in press
- Tinbergen J & Rutten R G M, 1992, A User Guide to WHT Spectropolarimetry, La Palma User Manual no 21. (Royal Greenwich Observatory)
- Whittet D C B, et al 1992, *ApJ*, **386**, 562

## Some general polarimetry texts and papers

- Clarke D. & Grainger J.F., 1971, *Polarized light and optical measurements* (Pergamon Press, Oxford)
- Collett E., 1993, *Polarized Light: Fundamentals and Applications* (Marcel Dekker, New York)
- di Serego Alighieri, S., 1996, *Polarimetry with Large Telescope*, in *Instrumentation for large telescopes*, VII Canary Islands Winter School of Astrophysics, ed. J M Rodriguez de Espinosa (CUP, in press)
- Planets, Stars and Nebulae Studied with Photopolarimetry*, ed. T Gehrels (University of Arizona Press, Tucson)
- Shurcliff W A, 1962, *Polarized light, Production and Use* (Harvard U. Press, Cambridge, MA)
- Tinbergen J., 1996, *Astronomical polarimetry*, (CUP)

## ANNEXE A: Scientific case for Gemini Polarimetry

Although the document is primarily concerned with the wavelength range 0.3 to 5 $\mu$ m, the scientific case does include the mid-infrared wavelengths.

### [A1] General

Polarimetry is a technique that can take particular advantage of the Gemini telescopes.

[A1.1] As degrees of polarisation are low (usually less than 5%), a large collecting area is needed to get the high signal to noise required for accurate polarimetry. Polarisation observations, especially in the optical and in the near-IR at moderate spectral resolution, are more likely to be source noise limited, with the limiting flux then scaling as the square of the telescope diameter, whereas the limiting flux scales as the telescope diameter for sky-limited observations. For example, with the NIRI, observations are source-noise limited at all wavelengths below 2 $\mu$ m, assuming an area of 0.25x0.25 arcsec<sup>2</sup> is used to calculate the polarisation, and all the source flux lies within it. At K, sources brighter than 0.1mJy will be source noise limited on Gemini (R=10, seeing 0.35 arc sec). Thus polarimetry will often have the same gains in using a larger telescope as high-resolution spectroscopy.

At mid-infrared wavelengths, the low emissivity of Gemini (with a goal ~8 times smaller than most other telescopes), combined with diffraction limited operation, gives a noise equivalent flux which is reduced by a factor of ~20 compared to observations on most 4m telescopes. To date, spectropolarimetry at these wavelengths is available on relatively few objects, often of the more extreme examples of a particular class of object, and hence statistics are very limited and can only be improved through polarimetry on very large telescopes.

A S/N ratio of 300:1 in total flux is required to achieve a 0.5% absolute uncertainty in the degree of polarisation. For the source-limited case this corresponds to 8x10<sup>4</sup> photons or 4x10<sup>4</sup> per Stokes parameter. Required accuracies vary considerably: a target of ~0.1% (absolute uncertainty) might be appropriate for velocity resolved spectropolarimetry of stars and AGN, whereas ~1% might be entirely adequate for reflection nebulae.

Following are a few examples of the sensitivities for a dual-beam polarimeter achieving a 0.5% accuracy in 1 hour of total integration time (15 min per wave-plate position for linear polarimetry). The polarimetry optics has been assumed to have a throughput of unity and any increased emission from the wave-plates has been ignored.

(i) **NIRI** (assuming the total throughput from atmosphere to electrons collected is 0.5, and a point source with all the flux contained within an area of 0.25x0.25 arcsec<sup>2</sup>): J-20.4, H-19.6, K-18.5, L-13.8 mag

(ii) **NIRS** (assuming the total throughput from atmosphere to electrons collected is 0.35, and a point source with double sampling of R=2000 in a 0.3 arc sec slit with 0.15 arcsec pixels): J-13.8, H-13.4, K-12.7, L-10.5 mag

(iii) **GMOS** (assuming the total throughput from atmosphere to electrons collected is 0.28, and a point source with a 0.5 arc sec slit, sampled by 0.08 arcsec pixels binned as 2x2; a spectral resolution of 2000 achieved with 3-pixel sampling, and pixels in the spatial direction co-added to include all of the flux): 0.4 $\mu$ m-13.9, 0.6 $\mu$ m-14.1, 0.8 $\mu$ m-13.5 mag

(iv) **HROS** (assuming the total throughput from atmosphere to electrons collected is 0.12, and a point source with  $R=50,000$  triple-sampled in a 0.6 arcsec slit): 0.4 $\mu$ m-9.5, 0.6 $\mu$ m-9.7, 0.8 $\mu$ m-9.1 mag

## [A2] Polarisation mechanisms and diagnostics

### [A2.1] Intrinsic mechanisms

**Cyclotron radiation**, which is circularly polarised, is produced by non-relativistic electrons spiralling in a large magnetic field. At low values of  $v/c$  most power is generated at the gyration frequency, while higher harmonics are produced as the velocity increases. High degrees of circular polarisation (up to  $\sim 50\%$ ), and lower degrees of linear polarisation, are produced in the AM Her binaries (polars), at optical and near-IR wavelengths. The polarised flux is produced by the streaming of matter from a red dwarf directly onto the surface of the white dwarf. Phase resolved polarimetry, both broadband and spectropolarimetry, can be used to determine the strength of the white dwarf magnetic field, and the geometry of the binary system including the accretion column (for a review see Cropper 1990).

**Synchrotron radiation**, which is linearly polarised, is produced by relativistic electrons in the presence of a magnetic field, and extends over the whole of the electromagnetic spectrum that is available from the ground. In some objects, such as the BL Lacertae, the synchrotron radiation dominates and polarisations as high as 50% can be produced for the unresolved source. In other objects, such as the Highly Polarised Quasars (HPQs), emission from the accretion disk, broad and narrow line gas, and hot dust, can also be observed, reducing the degrees of polarisation. Synchrotron radiation is produced by relativistic jets generated in the nuclei of active galactic nuclei (AGN) and this emission is doppler boosted when the jet is viewed end-on. The wavelength dependence of the polarised flux, particularly when combined with simultaneous observations at shorter wavelengths (from space) and submillimetre wavelengths can be used to understand the physics of the jets. Spectropolarimetry at optical and near-IR wavelengths can be used to study the interaction between the jet and gas in the AGN. For a recent review of radio-loud AGN see Urry (1995).

For a few objects the jet can be spatially resolved at optical and near-IR wavelengths (3C273, M87), providing the opportunity to study the evolution of the jet and acceleration mechanisms.

**Aligned dust grains** produce polarised radiation in emission. However, further discussion is left to the section on aligned grains under secondary mechanisms.

### [A2.2] Secondary mechanisms

**Scattering** of radiation from dust grains or free electrons occurs in many astrophysical situations, producing linear polarisation; circular polarisation can also be produced when polarised radiation is scattered from non-Rayleigh dust grains.

The polarised flux can be used to study regions which are normally obscured from direct view, and to study the geometrical and velocity relationship between the radiation source, scatterer and observer without spatially resolving the source. A comparison of total and (scattered) polarised flux provides views of a source from different angles.

Over the last decade spectropolarimetry has been used extensively in the study of Active Galactic Nuclei, showing that many have been wrongly classified and has thus led to the development of unified theories (see Antonucci 1993 for a useful review). It is now clear that

many AGN are surrounded by a geometrically and optically thick torus that can obscure our direct view of the nuclear regions. However, photons can escape along the poles of the torus, and then be scattered to us by electrons and/or dust revealing the nuclear spectrum in polarised flux.

Embedded young stars have similar geometries with the central object surrounded by a circumstellar disk, and larger interstellar disk, with the disk axes usually aligned with the bipolar outflows associated with all YSOs. The optical thickness of the disks, as viewed edge-on, is sufficiently high that at optical and near-IR wavelengths radiation from the central regions can only be observed in scattered light, with photons escaping along the disk poles, being scattered to us and forming the classical bipolar reflection nebulae. Linear polarisation provides information on the scattering geometries, including the geometry of the illuminating source, the inclination of the outflows, and the properties of the dust grains responsible for scattering the light to us. Circular polarimetry of the reflection nebulosity gives direct information on the geometry of the regions close to the central object, as the circular polarisation is produced by the scattering of radiation initially polarised in regions close to the central object.

High resolution spectropolarimetry of stars can be used to study the geometry of (aspherical) atmospheres, envelopes, and winds. Asymmetric winds have important implications for mass loss rates, and changes in QU space with time gives the physical changes in the distribution of scattering material, e.g. expansion, rotation. High spectral resolution is needed to study narrow features, perhaps associated with the motion of individual blobs of material.

**Aligned dust grains** can produce polarisation either in absorption or in emission. The spin axes of non-spherical dust grains can assume a preferred orientation through a variety of mechanisms. In the presence of a magnetic field the short axis of the grains will become aligned with the local magnetic field, producing polarisation in absorption which is parallel to the magnetic field, and in emission it is perpendicular to the magnetic field. Thus the position angle of polarisation gives directly the direction of the magnetic field projected onto the plane of the sky. Note that this yields information on the field component orthogonal to that provided from Zeeman splitting of spectral lines.

Polarimetry is a very important tool in determining the magnetic field structure close to young stars, in the disks and outflows associated with the early stages of stellar evolution and thus in testing the predictions of MHD theories of star formation.

At mid-IR wavelengths, both absorption and emission can occur, and their relative contributions can usually be determined by spectropolarimetry. Vibrational transitions in the solid state give rise to resonance features in the infrared, characteristic of the chemical bonds involved. These features are often polarised and the polarisation spectrum, unlike the intensity spectrum, is independent of the nature of the underlying source, so long as this is unpolarised. Even if this latter condition is not satisfied, polarisation in the underlying source, or variations in chemistry along the line of sight, are usually revealed by changes in position angle through the spectrum. Since the intensity and polarisation spectra are different functions of the optical constants of the grain material, spectropolarimetry gives additional and independent information about the physical and chemical structure of grains and their mantles. Finally, spectropolarimetry is a much more sensitive and independent probe of grain physics and chemistry than spectroscopy alone.

[A2.3] Disentangling mixed spectral components

Spectropolarimetry, and filter polarimetry over a wide-wavelength range, can be used to separate out different radiation components. For example, the polarised flux spectrum is independent of dilution from an unpolarised source. Even when there are 2 polarised components, these can be separated provided they have different spectral slopes and a different position angle of polarisation.

**[A3] Specific examples of polarimetry with Gemini**

[A3.1] Star formation

Star formation is a major unsolved problem in astrophysics and its early stages are often associated with the phenomena of bipolar flows. These are usually attributed to the presence of a disk or toroid of dust and gas close to the protostar that collimates its radiation and outflow. Studies of the polarisation of starlight on arc minute scales in the vicinity of the flows, or of distributed molecular hydrogen on arc sec scales (Hough et al 1986, Chrysostomou et al 1994), often reveals a magnetic field parallel to the flow direction. Conversely mid-IR spectropolarimetric studies of the central regions indicate a magnetic field which tends to be in the plane of the disk and normal to the larger scale field in the flow (Aitken et al 1993). These observations suggest that magnetic fields play a significant role in the star formation process but more detailed observations of more objects are required in order to develop a coherent understanding of their importance in star formation and early evolution.

Of the ten bipolar flows studied at mid-infrared wavelengths (Aitken et al 1993), all but one relate to regions of high mass star formation. That the magnetic field close to the star tends to be in the plane of the disk, is at variance with one of the more plausible and attractive hydromagnetic models of bipolar flows (Pudritz & Norman 1986) but the statistics are very limited and the spatial scale of the regions studied is poorly defined. These regions are distributed within the Galactic Plane and with Gemini's sensitivity there should be several hundred high-mass regions and many low mass regions available for study. Additionally the spatial structure and scales will be better defined and this can be augmented by polarimetric imaging for the highest spatial resolution.

Near-infrared imaging polarimetry has been used for some time to study the bipolar reflection nebulae associated with the outflows. Near to the source, the polarisation vectors are no longer in a centro-symmetric pattern, but form a band of aligned vectors known as "polarisation disks". For high-mass YSOs these disks are perhaps a 1000AU across and are presumably associated with the large-scale interstellar disks. Their origin, however, remains unclear and high resolution imaging polarimetry is needed to resolve any structure and to understand their origin and nature. While 4m class telescopes with AO might well be appropriate for these objects, the very high image quality projected for Gemini, and the low emissivity, will enable the smaller disks around more evolved young stars to be observed, particularly at the more difficult 2-5 $\mu$ m wavelength range. For example, VLA mm images of HL Tau show disk-like structures on a 1 arc sec size or 140AU, which are probably dusty accretion disks (Wilner, Ho & Rodriguez, 1996). Polarisation images can give information on the structures and composition (from scattering) and on the presence of magnetic fields from dichroism.

Circular polarisation images of the regions around YSOs is proving to be a very important diagnostic of the structure around the central object, and of the dust grains in the reflection nebula (Chrysostomou et al 1996a, Gledhill, Chrysostomou & Hough 1996). Circular polarisation is produced when linearly polarised radiation is scattered by non-Rayleigh dust

grains with an imaginary (absorptive) component to their refractive index. Thus circular polarisation gives the immediate polarisation history of photons, and gives information on the geometrical structures close to the source before photons are scattered to us. High spatial resolution is important so that circular polarisation structure close to the polarisation disks as well as in the reflection nebula can be determined.

#### [A3.2] Compact HII regions

Compact HII regions frequently show a component of polarised emission from warm dust grains, overlaid by absorptive polarisation. Polarised emission probes the fields within the ionised region and gives information about localised field components and their relation to the line of sight field revealed by the absorptive polarisation. Such studies can give important insights into some of the details of cloud collapse and subsequent evolution of the HII region, and since the ionised environment differs dramatically from that in molecular clouds, grains may be aligned by a different mechanism. The number of such sources available to Gemini would again be several hundred compared with about a dozen so far studied in spectropolarimetry. Here too there is great scope for polarimetric imaging to investigate detailed field morphology.

#### [A3.3] Circumstellar matter and asymmetric stellar envelopes

High-resolution spectropolarimetry of stars can be used to study the geometry of (aspherical) atmospheres, envelopes, and winds. Asymmetric winds have important implications for mass loss rates, and changes in QU space with time gives the physical changes in the distribution of scattering material, e.g. expansion, rotation. High spectral resolution is needed to study narrow features, perhaps associated with the motion of individual blobs of material.

During the early stages of a supernova explosion, circumstellar material becomes illuminated by the UV flash, giving rise to short-lived emission lines, of width  $\sim 10\text{km/s}$  (SN 1987A: Cummings & Meikle 1993). Spectropolarimetry of such features can provide information on the geometrical structure and expansion of this material

#### [A3.4] Chemical and physical properties of dust grains

Spectropolarimetry offers a less ambiguous and independent comparison of observations with laboratory studies than does spectroscopy alone. For instance polarisation spectra at 10 and  $20\mu\text{m}$  have been used to argue that the grains responsible for the extinction to the BN object consist of an amorphous silicate core with a refractory organic mantle, while in AFGL2591 they indicate that some of the silicate grains have undergone partial annealing (Aitken et al 1988). Very few polarisation studies have been done at  $20\mu\text{m}$  and Gemini should be well placed to increase this number to statistical significance. There are also at present only a small number of objects whose  $10\mu\text{m}$  polarisation spectra are not consistent with a generic silicate component, but even within this latter group there are significant variations of spectral form which indicate the physical state and history of the grain material. Only when the data base of these studies is increased significantly, as is possible with Gemini, can these differences be put into a detailed inventory of the solid component of the interstellar medium.

Near-infrared spectropolarimetry of the  $3\mu\text{m}$  ices-feature (Hough et al 1996 and references therein) has been shown to be an important diagnostic of the physical and chemical nature of dust grains, and the position angle of polarisation gives directly the direction of the local magnetic field. To date, relatively few lines of sight have been observed and to make further progress requires larger telescopes. Almost unexplored is the use of circular spectropolarimetry that is only possible for one or two sources with 4m class telescopes. Circular polarimetry is a very important diagnostic of grain chemistry being sensitive to the

imaginary component of grain refractive index, and to the twisting of magnetic fields along the line of sight.

Of particular importance is a comparison of the polarisation of the 3 $\mu$ m ice feature and the 10 $\mu$ m silicate feature, as this can provide information about the fractionation of ices along different lines of sight.

The mechanism by which grains align remains poorly understood, and one major problem is the apparent ability of grains to align in the cold dense parts of dark clouds. That such grains can align can be shown through spectropolarimetry of grains with a mantle of solid CO (wavelength of 4.67 $\mu$ m). Only one source has been observed with 4m telescopes (W33A - Chrysostomou et al 1996b), and only with 8m telescopes will a significant number of additional lines of sight be possible.

#### [A3.5] Solar system bodies

The polarisation of Solar System bodies can give information on the physics and chemistry of surfaces and sometimes of hot spots, such as volcanic flows, and may reveal the spin axes of unresolved bodies such as asteroids.

Since all of these studies concern solid state continua or features they would require relatively low resolving power, say  $R = 30-100$ , in both the near and mid-IR.

#### [A3.6] Galactic Centre

Studies of the Galactic Centre have revealed strong polarised emission from the warm dust grains within the ionised filaments in motion close to the non-thermal radio source SgrA\*. The magnetic fields indicated by polarimetric imaging in the mid-IR are highly organised with respect to the filaments and show structure at a one arcsecond scale (Aitken et al 1991) close to SgrA\* which would benefit from the higher spatial resolution attainable with Gemini at mid-IR wavelengths. The field directions in the Galactic Centre are thought to display the strain directions in the filaments and hence are directly related to their orbital motions. Since Gemini will be a very clean telescope polarimetric study of much lower surface brightness regions will be possible; this in turn can elucidate the relationship between the various filaments.

#### [A3.7] Active galaxies

Polarimetry has played a central role in our understanding of active galactic nuclei, from the study of blazars, with doppler boosted synchrotron emission, to radio-quiet Seyfert galaxies. For the latter class of object, optical spectropolarimetry has been instrumental in developing unified theories, with its ability to observe the central regions of the AGN, which may be hidden from our direct view by an optically and geometrically thick torus. Nuclear continuum and broadline photons can be scattered into our line of sight by electrons and or dust located along the polar axis of the torus.

While significant progress has been made there are a number of outstanding issues which will only be addressed with the larger aperture telescopes. They are:

(i) why do not all type II Seyferts have broadlines in their polarised flux spectrum? Either the broadlines do not exist (there really are type II Seyferts), or there is a dearth of scatterers close to the AGN, or the scattered radiation suffers significant extinction, or the scatterers are sufficiently hot to smear out the broadlines. Scattered broad infrared lines will of course be less attenuated, and therefore spectropolarimetry at near-infrared wavelengths may well pick

up many more hidden type I nuclei. However, the equivalent widths of scattered infrared lines is much lower than in the optical and only a handful of objects can be studied in this way with 4m telescopes. If the scattering occurs some distance from the AGN, then the amount of scattered flux will be small and again 8m telescopes will be needed to pick out the scattered broad lines.

(ii) Young et al (1995, 1996a) have proposed that the polarised flux for type II Seyferts, at near-IR wavelengths, arises mainly from a dichroic view, through the torus, of the hot dust responsible for the near-IR emission. If correct, this gives directly the direction of the magnetic field in the torus, important for understanding the way it formed and its dynamical stability. A prediction of this model is that the polarisation should change from being seen in absorption to emission, at a wavelength which depend on the optical depth of the torus. With 4m class telescopes, polarimetry beyond  $2\mu\text{m}$ , even at modest spectral resolution is very difficult for all but the few brightest Seyferts.

Spectropolarimetry of the silicate feature at  $10\mu\text{m}$  is a very important diagnostic of polarisation mechanisms, but with 4m telescopes this has been possible for just one object (NGC1068, Aitken et al 1984). In NGC1068 the polarisation is due to warm aligned dust grains, with the position angle of polarisation orthogonal to that at near-infrared wavelengths. On Gemini, the limiting flux for spectropolarimetry at  $10\mu\text{m}$  could well be at  $\sim 0.3\text{Jy}$  ( $\Delta p \sim 0.5\%$  in a few hours) at a resolving power  $R \sim 30$ , at which level a number of AGN become available for study. Thus, spectropolarimetry, through its ability to detect solid state spectral features, should be able to discriminate between thermal and non-thermal emission in other AGN's.

(iii) do the NLRGS all have hidden broad lines? To date, only three NLRGs have been observed to have broadlines in their polarised flux spectrum (Young et al 1996b, and references therein). The radio galaxies are much fainter than the Seyferts, and hence 4m telescopes are adequate for just a few objects. Also, it is possible that in a number of NLRGs (e.g. CenA, Packham et al, 1996) scattered nuclear radiation suffers significant extinction and therefore broadlines will only be observed at near-infrared wavelengths.

(iv) a number of type II Seyferts have been observed to have broad lines in their total flux spectrum at infrared but not at optical wavelengths. This has been used to estimate the extinction through the torus, although it is not known in most cases whether the broadline component has been scattered to us rather than observed directly. Young et al (1996c) has shown that scattering does indeed dominate, in at least one case, leading to much higher estimates of the optical thickness of the torus. Unfortunately infrared spectropolarimetry can only be carried out on a few objects with 4m class telescopes.

(v) the physical nature of the Broad Absorption Line quasars is still poorly understood, and 4m class telescopes have not been able to provide the polarisation accuracy, particularly in the deep absorption troughs, to construct consistent models of these systems.

(vi) space missions, such as ISO, will identify new heavily obscured, high-z, AGN. Spectropolarimetry, at both optical and near-infrared wavelengths on 8m telescopes will be needed to identify the true nature of the nuclear sources.

(vii) the well-known "alignment effect" in high-z radio galaxies (McCarthy et al 1987, Chambers, Miley & van Breugel 1987), in which line and continuum emission is aligned with the radio emission has been studied for some time. Explanations range from star formation induced by the jet (Rees 1989), to scattering of nuclear radiation by electrons and/or dust (Tadhunter, Fosbury & di Serego Alighierei 1989). Radio galaxies with  $z > 0.7$  have V magnitudes fainter than 20, and so high accuracy spectropolarimetry and imaging polarimetry

requires larger telescopes. The spectropolarimetry is essential to identify and remove the AGN contribution for very distant radio galaxies, so that their stellar evolution can be studied in detail.

- Aitken D K, et al 1984. *Nature*, 310, 660.  
Aitken D K, et al 1988. *MNRAS*, 230, 629.  
Aitken et al 1991, *MNRAS*, 380, 419  
Aitken et al 1993, *MNRAS*, 262, 456  
Antonucci R R J, *Unified Models for Active Galactic Nuclei and Quasars*, Annual Reviews of Astronomy & Astrophysics, 1993  
Chambers K C, Miley G K & van Breugel W, 1987, *Nature*, 329, 604  
Chrysostomou A, et al 1996a (circular)  
Chrysostomou A, et al 1996b (W33A)  
Chrysostomou A, et al 1994. *MNRAS*, 268, 325.  
Cropper M, 1990 *Space Science Review* 54, 195  
Cummings RJ & Meikle WPS, 1993, *MNRAS*, 262, 689  
Gledhill, Chrysostomou & Hough 1996 (circular)  
Hough et al 1986. *MNRAS*, 222, 629.  
Hough J H, et al 1996. *Ap J.*, 461, 902  
McCarthy et al 1987, *ApJ*, 321, L29  
Packham C, et al 1996. *MNRAS*, 278, 406-416  
Pudritz & Norman 1986, *ApJ* 301, 571  
Rees M, 1989, *MNRAS*, 239, 1p  
Tadhunter C N, Fosbury R A E, di Sergio Alighieri S, 1988. In "BL Lac Objects" Maraschi L, Maccacaro T & Ulrich M-H, eds Springer-Verlag, Berlin p79  
Urry C M, 1995, *PASP*, 107, 803  
Wilner, Ho & Rodriguez, 1996. *ApJ*, 470, L117  
Whittet D C B, et al 1992, *ApJ*, 386, 562  
Young S, et al 1995. *MNRAS*, 272, 513  
Young S, et al 1996a, *MNRAS*, 281, 1206  
Young S, et al 1996b. *MNRAS*, 279, L72  
Young S, et al 1996c. *MNRAS*, 280, 291

## **ANNEXE 2: Alternative modulators**

Alternative variable retarders are Pockels Cells, Photoelastic Modulators and Liquid Crystals, and brief descriptions of these are given below. All these devices use electrical voltages to change the retardance. However, to measure more than one Stokes parameter either two retarders need to be used in series or a waveplate is introduced or in some cases the cells can be rotated. The latter two options involve a mechanical change and thus negates what is often seen as the advantage of electrically driven variable retarders, namely the lack of image wander that can result when an optical element is introduced or is rotated.

The possibility of not using any retarder is also discussed.

#### [A2.1] Pockels Cells

These have been used in a number of systems with photon counting detectors (e.g. McLean et al 1984). By the application of a switching high voltage, the cell (usually made of the electro-optic crystal KD\*P) can be made to operate as a reversible retarder. In order not to damage the Pockels cell the EHT has to be switched at a rate of 1Hz, or faster, and hence cannot be used with array detectors where readout noise is likely to dominate for small exposures, or where the readout time is long compared to the period of the cell switching time. Further disadvantages are that the Cell cannot be made achromatic and is therefore retuned for different wavelengths and they are usually used in a collimated beam as the polarisation efficiency drops quickly with the angle of incidence.

#### [A2.2] Photoelastic modulators (PEM)

A piezotransducer is used to produce a longitudinal oscillation in a slab of material, such as fused silica, leading to a time-varying stress birefringence (Kemp 1969). The PEM then functions as a variable retarder. The PEM is an excellent modulator having high transmission over a large wavelength range and can accept large angular beams. Like the Pockels Cell, the PEM cannot be constructed in achromatic form but can easily be tuned in wavelength. The natural frequency of oscillation of the crystals is, however, very high (~10kHz), making them unsuitable for use with array detectors which have far slower frame rates. It is possible to use a slow modulation by using the beat frequency of two crystals with nearly equal oscillation frequencies (Stenflo & Povel 1985), however, the modulation efficiency is then low.

#### [A2.3] Liquid Crystals

Recently available commercially is the Meadlowlark liquid crystal with electrically adjustable retardance. It has a large acceptance angle and the transmission can be in excess of 92% in the visible and near-infrared. The use of two cells enables both linear Stokes' parameters to be determined without any mechanical rotation. A system has been tested at the University of Glasgow (R Smith, PhD Thesis), but it appears that the modulation efficiency is sensitive to the actual spectral pass-band making the device unattractive for spectropolarimetry. The retardance of the cell is also a function of temperature, although the latest devices have inbuilt temperature control with the cell voltage automatically keeping the retardance fixed. The maximum aperture is only ~30mm and generally the liquid crystal retarders appear to have little merit for most astronomy applications.

#### [A2.4] Instrument rotation

An alternative mode of operation, that can be used in imaging mode, is to rotate the instrument through 45° steps. This has the advantage that an upstream retarder is not required for modulation of the polarised signal, and instruments could be used on the side-ports, but this is at the expense of a reduced precision in the measured degree of polarisation that can be attained, as the image will rotate on the array.

### References

- McLean et al, 1984, MNRAS, **209**, 655  
Kemp J. C. 1969, J. Opt. Soc. Am., **59**, 950-4  
Stenflo & Povel, 1985, Applied Optics, **24(2)**, 3893



### ANNEXE 3: Materials for analysers

At optical wavelengths either calcite blocks (or Savart plates) or Wollaston prisms made from magnesium fluoride have been used. At near-infrared wavelengths cemented Wollaston prisms made from magnesium fluoride and lithium niobate have been used at the AAT and at UKIRT.

A new material,  $\alpha$ -BBO (Barium Borate) is being used for a Wollaston prism for UFTI, a new IR imager at UKIRT.

Soft cements are available for prisms to be used at low temperatures ( $\sim 80\text{K}$ ), although companies will not guarantee their performance for prisms with widths more than  $\sim 25\text{mm}$ . The cut angle of the prism is limited for uncemented prisms because of total internal reflection.

Often space for analysers is very limited and thus materials with a high birefringence are attractive. However, the birefringence may be strongly wavelength dependent and lead to elongation of images in the polarisation dispersion direction (lateral chromatism), although this will be less of a problem for spectrometers. Calcite has a high birefringence and lateral chromatism but has been used in several optical spectrometers. It can be used from  $0.3$  to  $2.2\mu\text{m}$ . Its high coefficient of thermal expansion makes it unattractive for use as a cemented Wollaston at low temperatures.

Magnesium fluoride has many ideal properties, being readily available, and having excellent transmission from the  $0.3$  to  $6\mu\text{m}$ . However, its birefringence is very small, and either large prisms have to be made or small separations have to be tolerated.

$\text{LiNbO}_3$  has the advantage of a much larger birefringence and so much thinner prisms can be used. It is readily available and can be made in sizes up to  $\sim 70\text{mm}$ , however, cemented prisms used at low temperatures are not guaranteed for prisms wider than  $\sim 25\text{mm}$ . It has a large refractive index (2.24), so requires AR coatings, and the birefringence is moderately wavelength dependent. Oliva et al (1996) discuss two materials which have both high birefringence and low lateral chromatism. Silver thiogallate ( $\text{AgGaS}_2$ ) has a birefringence at  $1.6\mu\text{m}$  which is  $\sim 5$  times that of  $\text{MgF}_2$ , but with a lateral chromatism which is a factor of two lower. However, the refractive index is high (2.46) and  $\text{AgGaS}_2$  crystals are significantly deformed by cooling. A second material, YLF ( $\text{LiYF}_4$ ), is transparent to beyond  $4\mu\text{m}$ , its birefringence at  $1.6\mu\text{m}$  is twice that of  $\text{MgF}_2$  and its lateral chromatism is lower by a factor of  $\sim 12$  (although this reduces to a factor of only two better at  $2.2\mu\text{m}$ ). As its refractive index is only 1.45, and the crystals are only slightly deformed by cooling, YLF could be an ideal material for Wollaston prisms in the near-infrared. However, it is a very difficult material to purchase and it appears that it has not been used to date.

A synthetic material that can be obtained, possibly up to  $40\text{mm}$  sides, and has attractive properties from the optical to  $\sim 2\mu\text{m}$ , is  $\alpha$ -BBO. It has a very high birefringence and relatively low lateral chromatism below  $1\mu\text{m}$  and very low from  $1$  to  $2\mu\text{m}$ <sup>1</sup>. It does, however, have a slight absorption at  $2.3\mu\text{m}$ , and cannot be used beyond the K-band.

<sup>1</sup> An  $\alpha$ -BBO prism purchased for UFTI (UKIRT) has a wavelength dependence of birefringence that is 10 x the expected value.

Tables and plots of birefringences for a number of materials are given below. Also included in the tables are the percent changes in birefringence per  $\mu\text{m}$ . The actual image elongation, due to lateral chromatism, is given by (fractional change in birefringence per micron) x

(passband in microns) x (separation of e and o beams). Care should be exercised in using these tables as data from different sources are not always in very good agreement. This may arise from the different ways crystals have been produced. First, a summary table of the birefringences and its percentage change at a number of wavelengths is presented followed by recommendations on the type of analyser that might be used for Gemini instruments.

$n_e - n_o$ / %change	$\lambda \mu\text{m}$	0.8	1.2	1.6	2.0	2.4	2.8	3.2	3.6
MgF <sub>2</sub>	0.012 -14	0.012 -6	0.0115 -3.0	0.011 -2.0	0.011 -3.0	0.011 -5.0	0.011 -4.0	0.011 -8	0.010 -9
YLF	0.024 -26	0.022 -4.2	0.022 -1.3	0.022 -0.40	0.022 2.9	0.022 2.9			
LiNbO <sub>3</sub>	0.107 -115	0.079 -17	0.075 -6	0.073 -10	0.071 -5.2	0.068 -7.	0.067 -14	0.063 -16	0.062 -17
$\alpha$ -BBO <sup>1</sup>	0.147 -34	0.138 -3.2	0.138 0.80	0.138 1.0	0.139 3.7				
Calcite	0.24 -52	0.22 -6.8	0.21 -9	0.20 -7	0.196 -13				

<sup>1</sup> An  $\alpha$ -BBO prism purchased for UFTI (UKIRT) has a wavelength dependence of birefringence that is 10 x the expected value.

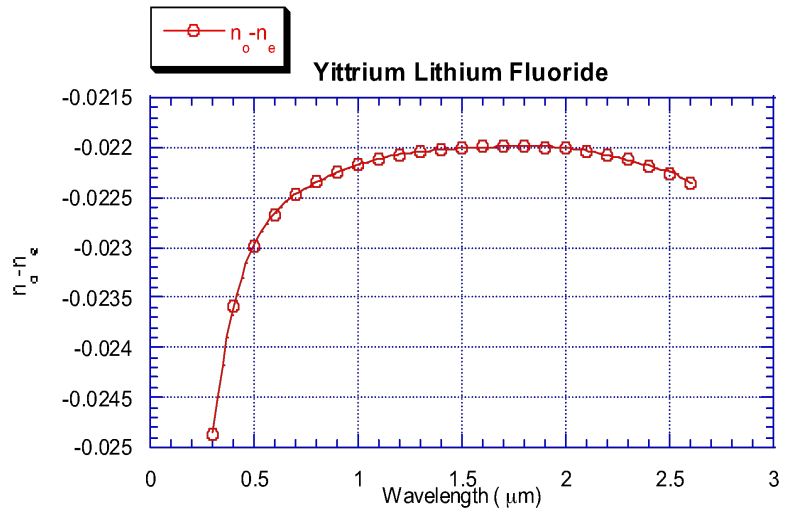
Possible recommendations for Gemini instruments:

- (i) **GMOS** - use a magnesium fluoride Wollaston prism. B Halle will make a composite of 4 prisms of sufficient clear aperture for the collimated beam. Although the separation of beams will be modest (~20 arcsec), the big advantages over a below the slit calcite are: availability, no need to have a focus adjust when the Wollaston is deployed, and can be used with an image-slicer IFU.
- (ii) **HROS** - probably a Savart plate but needs to be looked at again
- (iii) **NIRI** - recommend an  $\alpha$ -BBO Wollaston prism<sup>1</sup> for the JH & possibly the K band, but for longer wavelengths use Lithium Niobate or Magnesium Fluoride, but the latter will only give small separations.
- (iv) **NIRS** - as for NIRI

<sup>1</sup> An  $\alpha$ -BBO prism purchased for UFTI (UKIRT) has a wavelength dependence of birefringence that is 10 x the expected value.

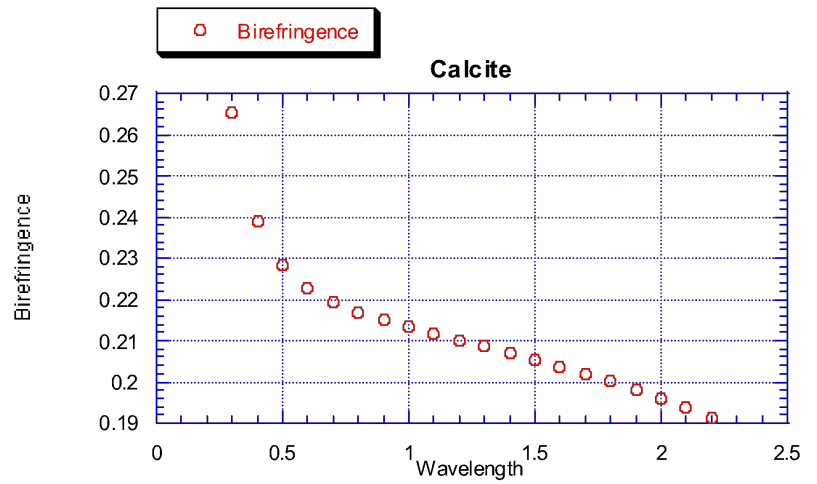
**Birefringence for Yttrium Lithium Fluoride (values taken from a Dispersion Formula - Table 22 of the Handbook of Optics, 2<sup>nd</sup> edition). Refractive index ~1.45.**

$\lambda(\mu\text{m})$	$n_o-n_e$	% change per $\mu\text{m}$
0.30	-0.024866	-50.298
0.40	-0.023580	-26.861
0.50	-0.022988	-14.109
0.60	-0.022664	-8.0063
0.70	-0.022466	-5.4277
0.80	-0.022334	-4.2698
0.90	-0.022241	-3.4990
1.0	-0.022172	-2.7442
1.1	-0.022119	-1.9864
1.2	-0.022078	-1.3196
1.3	-0.022045	-0.83940
1.4	-0.022020	-0.58229
1.5	-0.022002	-0.47692
1.6	-0.021990	-0.40221
1.7	-0.021984	-0.22575
1.8	-0.021985	0.14107
1.9	-0.021993	0.70874
2.0	-0.022010	1.3730
2.1	-0.022035	1.9569
2.2	-0.022071	2.3124
2.3	-0.022119	2.4619
2.4	-0.022179	2.8692
2.5	-0.022255	4.7692
2.6	-0.022347	



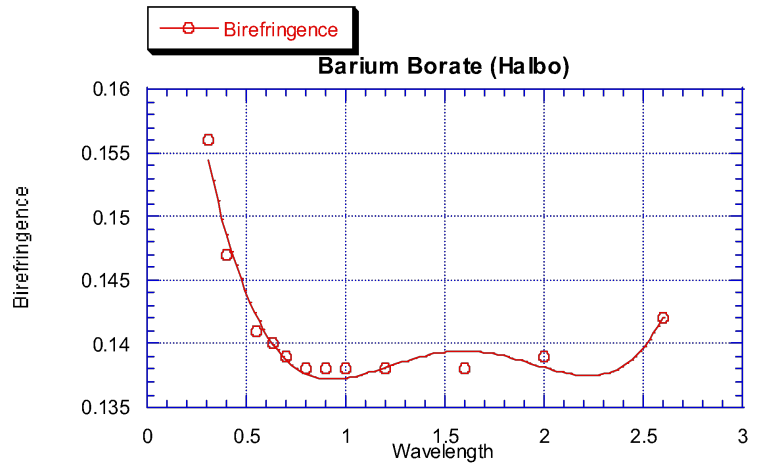
**Birefringences for calcite (values taken from a Dispersion Formula - Table 22 of the Handbook of Optics, 2<sup>nd</sup> edition). Refractive index ~2.2**

$\lambda(\mu\text{m})$	$n_o-n_e$	% change per $\mu\text{m}$
0.30	0.26532	-89.595
0.40	0.23890	-52.628
0.50	0.22842	-27.653
0.60	0.22290	-13.802
0.70	0.21943	-7.9649
0.80	0.21694	-6.8035
0.90	0.21496	-7.6536
1.0	0.21324	-8.7883
1.1	0.21166	-9.3190
1.2	0.21013	-8.9912
1.3	0.20860	-8.0275
1.4	0.20704	-6.9625
1.5	0.20543	-6.4174
1.6	0.20373	-6.9058
1.7	0.20195	-8.6346
1.8	0.20006	-11.236
1.9	0.19806	-13.570
2.0	0.19592	-13.451
2.1	0.19365	-7.2955
2.2	0.19123	



**Birefringences for  $\alpha$ -BBO<sup>1</sup> (Values supplied by Halbo Optics). Refractive index ~1.6.**

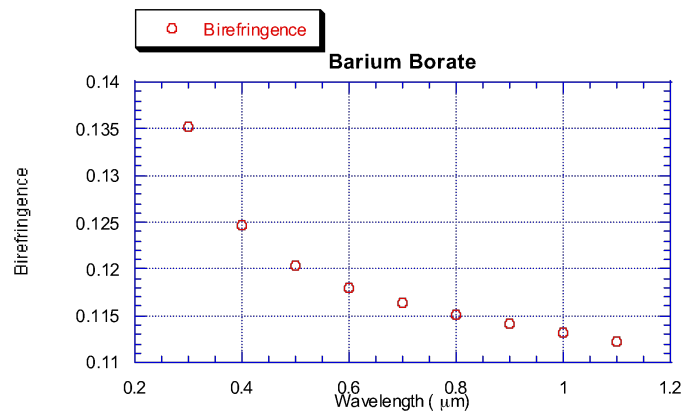
$\lambda(\mu\text{m})$	$n_o-n_e$	% change per $\mu\text{m}$
0.31	0.15600	-41.4
0.40	0.14700	-29.0
0.55	0.14100	-19.0
0.63	0.14000	-13.3
0.70	0.13900	-7.9
0.80	0.13800	-3.0
0.90	0.13800	0.44
1.0	0.13800	
1.1		3.0
1.2	0.13800	
1.5		2.3
1.6	0.13800	
1.9		-2.3
2.0	0.13900	
2.5		4.7
2.6	0.14200	



<sup>1</sup> An  $\alpha$ -BBO prism purchased for UFTI (UKIRT) has a wavelength dependence of birefringence that is 10 x the expected value.

**Birefringences for  $\alpha$ -BBO<sup>1</sup> (values taken from a Dispersion Formula - Table 22 of the Handbook of Optics, 2<sup>nd</sup> edition)**

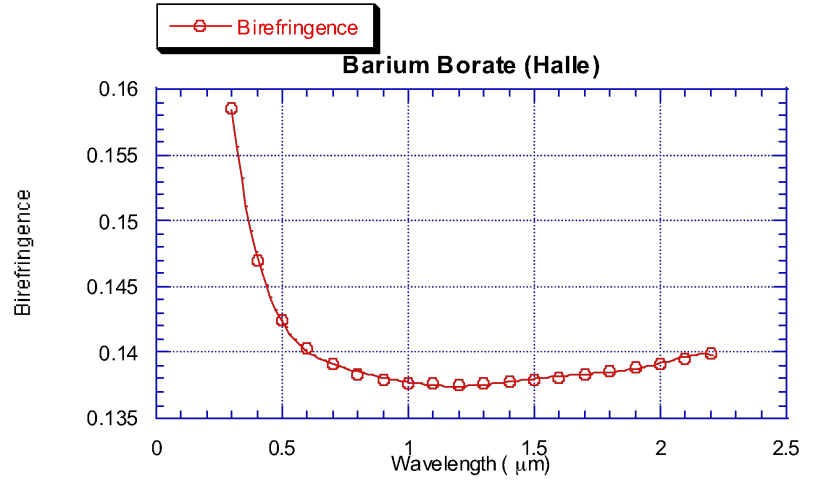
$\lambda(\mu\text{m})$	$n_o-n_e$	% change per $\mu\text{m}$
0.30	0.13521	-78.202
0.40	0.12463	-34.473
0.50	0.12034	-19.610
0.60	0.11798	-13.352
0.70	0.11641	-10.459
0.80	0.11519	-9.0610
0.90	0.11414	-8.4659
1.0	0.11318	-8.3013
1.1	0.11224	



<sup>1</sup> An  $\alpha$ -BBO prism purchased for UFTI (UKIRT) has a wavelength dependence of birefringence that is 10 x the expected value.

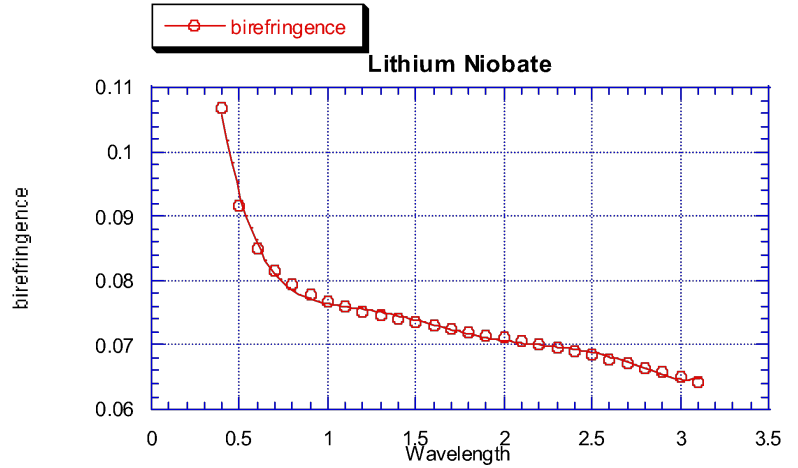
**Birefringences for  $\alpha$ -BBO (values taken from a Dispersion Formula supplied by B Halle, good from 0.2 to 2 $\mu$ m)**

$\lambda(\mu\text{m})$	$n_o-n_e$	% change per $\mu\text{m}$
0.30	0.15848	-69.369
0.40	0.14697	-34.659
0.50	0.14249	-15.441
0.60	0.14029	-6.9711
0.70	0.13907	-4.0412
0.80	0.13836	-3.1912
0.90	0.13795	-2.6028
1.0	0.13771	-1.6464
1.1	0.13761	0.39460
1.2	0.13759	0.79287
1.3	0.13764	1.5498
1.4	0.13775	1.7193
1.5	0.13790	1.4291
1.6	0.13810	1.0473
1.7	0.13832	1.0500
1.8	0.13858	1.7701
1.9	0.13887	3.0229
2.0	0.13918	3.6691
2.1	0.13952	1.0594
2.2	0.13988	



**Birefringences for Lithium Niobate (values taken from a Dispersion Formula - Table 22 of the Handbook of Optics, 2<sup>nd</sup> edition; is also values used by B Halle). Refractive index ~2.2.**

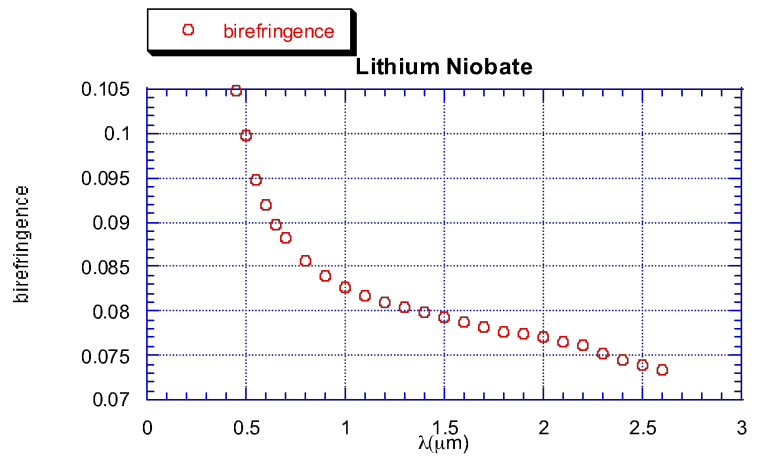
$\lambda(\mu\text{m})$	$n_o-n_e$	% change per $\mu\text{m}$
0.40	0.10690	-115.75
0.50	0.091565	-82.999
0.60	0.085025	-54.326
0.70	0.081499	-31.931
0.80	0.079317	-17.494
0.90	0.077828	-9.2452
1.0	0.076733	-5.6194
1.1	0.075876	-5.0851
1.2	0.075167	-6.0965
1.3	0.074554	-7.6885
1.4	0.074003	-9.0735
1.5	0.073491	-9.8906
1.6	0.073001	-9.9494
1.7	0.072523	-9.2775
1.8	0.072049	-8.0734
1.9	0.071571	-6.5864
2.0	0.071086	-5.2591
2.1	0.070588	-4.4055
2.2	0.070075	-4.3386
2.3	0.069544	-5.2420
2.4	0.068991	-7.0859
2.5	0.068415	-9.7205
2.6	0.067814	-12.478
2.7	0.067185	-14.517
2.8	0.066527	-14.378
2.9	0.065837	-9.9997
3.0	0.065114	1.1494
3.1	0.064355	
3.6	0.0616	17



NB The values for 3.6 $\mu\text{m}$  are taken from the IRCAM data using the measured change in beam separation relative to 1.2 $\mu\text{m}$ .

**Birefringences for Lithium Niobate (values taken from Handbook of Optics, Table 15, earlier edition)**

$\lambda(\mu\text{m})$	$n_o-n_e$	% change per $\mu\text{m}$
0.4500	0.10490	-86.531
0.5000	0.099800	-75.469
0.5500	0.094700	-64.873
0.6000	0.091900	-54.520
0.6500	0.089800	-45.334
0.7000	0.088200	-33.393
0.8000	0.085700	-21.256
0.9000	0.084000	-13.115
1.0000	0.082700	-8.2765
1.1000	0.081800	-5.9645
1.2000	0.081000	-5.4306
1.3000	0.080400	-5.9219
1.4000	0.079800	-6.8450
1.5000	0.079300	-7.7347
1.6000	0.078800	-8.2770
1.7000	0.078200	-8.2758
1.8000	0.077700	-7.6981
1.9000	0.077400	-6.6637
2.0000	0.077100	-5.4661
2.1000	0.076600	-4.5383
2.2000	0.076100	-4.5375
2.3000	0.075200	-6.2468
2.4000	0.074400	-10.675
2.5000	0.073900	-18.955
2.6000	0.073300	-23.769



**Birefringences for magnesium fluoride (values taken from Dodge 1984, AppliedOptics, 23, No12, page 1980). Refractive index ~1.35.**

$\lambda(\mu\text{m})$	$n_o-n_e$	% change per $\mu\text{m}$
0.3000	0.012500	-15.730
0.3500	0.012200	-14.458
0.4000	0.012070	-13.252
0.4500	0.012000	-12.114
0.5000	0.011900	-11.043
0.5500	0.011850	-10.040
0.6000	0.011800	-9.1051
0.6500	0.011770	-8.2363
0.7000	0.011740	-7.0516
0.8000	0.011680	-5.7038
0.9000	0.011650	-4.5956
1.0000	0.011610	-3.7110
1.4000	0.011470	-2.0428
1.8000	0.011320	-2.4670
2.2000	0.011140	-3.9426
2.6000	0.010940	-6.2166
3.0000	0.010680	-7.5222
3.4000	0.010400	-8.3471
3.8000	0.010080	-8.8511
4.2000	0.0097100	-9.5661
4.6000	0.0092900	-11.488
5.0000	0.0088400	-16.233

